A Soft Computing Approach for Rainfall Retrieval From the TRMM Microwave Imager

Diganta Kumar Sarma, Mahen Konwar, Jyotirmoy Das, Srimanta Pal, and Sanjay Sharma

***Abstract*—A neural network model for rainfall retrieval over ocean from remotely sensed microwave (MW) brightness temperature (BT) is proposed. BT data are obtained from the Tropical Rainfall Measuring Mission (TRMM) Microwave Imager (TMI). The BT values from different channels of TMI over the Pacific Ocean (163° tto 177°W and 18° to 34°S) are the input features. The near-surface rainfall rate from the Precipitation Radar (PR) are considered as a target. The proposed model consists of a neural network with online feature selection (FS) and clustering techniques. A K-means clustering algorithm is applied to cluster the selected features. Different networks have been trained to give an instantaneous rainfall rate with all input features as well as with selected features obtained by applying the FS algorithm. It is found that the hybrid network utilizing FS and clustering techniques performs better. The developed network is also validated with two independent datasets on March 14, 2000 over the Atlantic Ocean having stratiform rain and on March 21, 2000 over the Pacific Ocean having both stratiform and convective rain. In both cases, the hybrid network performs well with correlation coefficient improving to 0.78 and 0.81, respectively, in contrast to 0.70 and 0.75 for the network with all features. The rainfall rate retrieved from the hybrid network is also compared with the TMI surface rain rate, and a correlation of 0.84 and 0.75 is found for the two events. The proposed hybrid model is validated with a Doppler Weather Radar, and correlation of 0.52 is observed.**

***Index Terms*—Backpropagation, clustering, feature selection, microwave brightness temperature, modeling, neural networks, satellite rainfall estimation.**

I. Introduction

RAINFALL is a highly discontinuous process both in space and time. An accurate and reliable measurement of global rainfall is still a formidable challenge to meteorologists. Though from all the *in situ* measurements rainfall rate can be retrieved over a comparatively large area, still they cover only a small fraction $(<10\%)$ of the globe. The remote sensing techniques from space have the potential of providing global rainfall information. It can be classified broadly into empirical and physical basis approaches with a range of wavelengths from visual (VIS) and infrared (IR) to the microwave (MW) regime. The Tropical Rainfall Measuring Mission (TRMM) Microwave Imager (TMI) and Precipitation Radar (PR) on the same platform of TRMM covering a common swath, provides an excellent opportunity to study the global precipitation and also the instantaneous rainfall rate. At passive MW frequencies, precipitation particles are the main sources of attenuation of upwelling radiation. Therefore, MW techniques are physically more direct than those based on VIS/IR radiation. The observed brightness temperature (BT) of upwelling radiation at different frequencies depends upon the type and size of the detected hydrometeors. Upwelling radiations at high MW frequencies (50–100 GHz) are scattered by the raining system, leading to reduction in the observed BT of the Earth's surface. At lower frequencies (<50 GHz) the absorption/emission property is the primary mechanism affecting the transfer of MW radiation, where the ice particles above the rain layer are virtually transparent. The sea surface has a low emissivity (~ 0.4), whereas raindrops are much more effective emitter, thus providing a good contrast against the sea surface.

Many authors have demonstrated the combined use of MW and IR data for rainfall estimation using different methods, e.g., see [1] and [2]. Artificial neural network (ANN) techniques are also widely used for rainfall retrieval. More recently, use of ANN for real-time rainfall estimation using Meteosat satellite data is manifested by Grimes *et al.* [3]. They also showed the use of the principal component analysis (PCA) to reduce the data volume and of a pruning technique to identify the redundant input data. Hsu *et al.* [4] showed the use of an adaptive ANN model that estimates rainfall rates using IR satellite imagery and ground–surface information. Better performance of the ANN approach over linear regression for rainfall estimation over ocean is demonstrated by Tsintikidis *et al.* [5] from Special Sensor Microwave/Imager (SSM/I) MW data, whereas Bellerby *et al.* [6] manifested the consistently better performance of an ANN over locally calibrated Geostationary Operational Environment Satellite (GOES) Precipitation Index (GPI) technique. They utilized the database of the brightness temperature and their spatial derivatives for three IR and one VIS sensor on the GOES geostationary satellite.

In this paper, a soft computing approach for rainfall rate estimation over ocean is studied using online feature selection, clustering, and hybrid neural network. The inputs in terms of BTs are provided from the different channels of TMI, ranging from 10.67–85.5 GHz. The collocated PR rainfall rate is considered as the target values. The present study can be organized as follows. Section II describes the satellite systems and the preparation of the dataset. The methodology and a general background of the ANN, the feature selection technique, and the clustering algorithm are discussed in Section III. The overall training and

Manuscript received November 18, 2004; revised April 29, 2005. This work was supported by the Department of Space, Government of India under the RESPOND Program.

D. K. Sarma and M. Konwar are with the Kohima Science College, Nagaland 797002, India.

J. Das and S. Pal are with the Electronics and Communication Sciences Unit, Indian Statistical Institute, Kolkata 700108, India.

S. Sharma is with the Department of Physics, Kohima Science College, Nagaland 797002, India (e-mail: sanjay_sharma11@hotmail.com).

Digital Object Identifier 10.1109/TGRS.2005.857910

validation results are presented in Section IV. Section V is comprised of case studies on two rain events. Discussion and conclusions of the results are presented in Section VI.

II. Satellite System and Data Preparation

The TRMM satellite, carrying five sensors, was originally put in a 350-km circular orbit with an inclination angle of 35°, and it was boosted to 402.5-km orbit after August 14, 2001. The TMI and PR sensors are of interest in the present study.

The scanning geometries of TMI and PR are different. PR is a nadir-looking active sensor, and it performs a cross-track scanning, whereas TMI has a conical scan with a viewing angle of 49° off nadir (i.e., 52.8° incident angle). As the TMI is rotating while its receiver is integrating, the concept of effective field of view (EFOV) has been introduced. It is the effective area swept by the antenna beam during the integration time. The EFOV along the cross-track direction has sizes of 9.1 km for all the lower channels and 4.5 km for the 85-GHz channel. This artificially narrow EFOV-CT gives the value of BTs. Detail descriptions of the configuration of the TRMM instrument package can be found in Kummerow *et al.* [7].

The raw data from the different sensors are treated through different algorithms to obtain useful TRMM products designated as "TRMM standard data products." Three of these products are utilized for the present study. These are referred as 2A25; PR rain rate/PR-corrected reflectivity, 1B11; TMI Brightness Temperature (1B11), and 2A12; TMI surface rain rate and the vertical profiles of hydrometeors. These standard products are of version 5. We have considered in our case the near-surface rainfall rate, which is defined as the rainfall rate at the lowest height free from ground clutter. The vertical profile in 2A12 data product consists of 14 layers up to 18 km in heights, which are calculated by standard algorithms developed by Kummerow *et al.* [8]. As the sea surface has emissivity ~ 0.4 and land has high emissivity ~ 0.8, the TMI-2A12 algorithm uses different algorithms over ocean and land.

Being on the same platform, TMI and PR covers a common swath of scanning of ~ 200 km. Within this common swath there are pixels of PR which are nearer or overlapped with TMI pixels. The platform allows quantitative collocated comparisons of rain estimates from the two sensors. These collocated measurements from these two sensors have provided the most comprehensive dataset. As TMI and PR take samples at nearly the same time (where the time difference is approximately 1 min), this can be ignored as the observed precipitation system remains nearly stationary for this period [9]. In order to find the collocated pixels of both TMI and PR, we have chosen latitude and longitude difference of $\pm 0.04°$ between all the nine channels of TMI and PR. For lower frequency channels, as the EFOV-CT is of size 9.1 km, two PR pixels are averaged. For the 85-GHz channel, the footprints are approximately of same size of PR. Therefore, two consecutive pixels of TMI and PR are averaged. In the present study, BT data are collected over the Pacific Ocean covering an area between 163° to 177°W and 18° to 34°S. BT values corresponding to both stratiform and convective type of rain are incorporated in the training dataset.

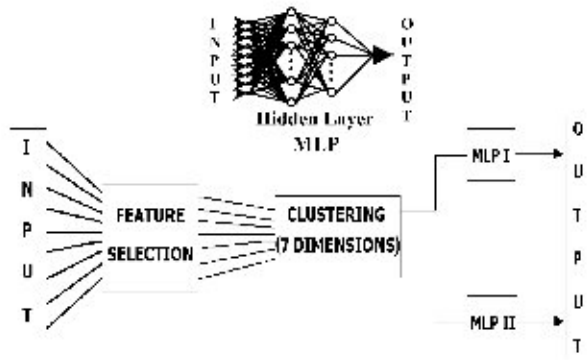

Fig. 1. Schematic diagram of the methodology.

III. Methodology

In the present study, we have applied an online feature selection (FS) algorithm to the BT dataset obtained from TMI. The nine-channel BT data are the input feature to this feature selection algorithm. It selects the most relevant channels both vertical as well as horizontal. A k-means clustering algorithm is then applied to the dataset of selected features. Separate multilayer perceptron (MLP) neural networks are trained for each of the clustered data. These trained MLPs are then combined to form a hybrid network. The schematic diagram of the methodology is shown in Fig. 1.

A. MLP Neural Network

The MLP network consists of several layers of neurons of which the first one is the *input layer* and the last one is the *output layer*, and the in-between layers are called *hidden layers* [10]. Every node, except the input layer nodes, computes the weighted sum of its inputs and applies an activation function, a sigmoid function to compute its output. This output is then transmitted to the nodes of the next layer. The objective of the MLP learning is to set the connection weights in such a manner so as to minimize the error between the network output and the target. For the present study, the backpropagation gradient decent method of learning is utilized.

B. Online Feature Selection Technique

The main objective of the *online feature selection* network is to select the good features for learning the estimation task. In a standard MLP, the effect of some features (inputs) can be eliminated by not allowing them to enter into the network [11]. This can be realized by associating an adaptive gate to each input node of the MLP. This feature selection network is known as FSMLP. Mathematically, the gate is modeled by a function F with a tunable parameter (γ). The degree to which the gate is opened determines the goodness of the feature. The gate should be modeled in such a way that it is completely opened for a good feature, with the value of the function must be nearer to 1. While for a bad feature, the gate should be closed, which means the value of the function is near about 0. On the other hand, for a partially important feature, the gate could be partially open, with the value of the function between 0 and 1. We multiply an input

TABLE I
ATTENUATION WEIGHT VALUES FOR NINE—INPUT FEATURES

FEATURES	ATTENUATION WEIGHTS	REMARKS
Channel 1	0.9928	Accepted
Channel 2	0.9451	Accepted
Channel 3	0.9899	Accepted
Channel 4	0.9978	Accepted
Channel 5	0.0025	Rejected
Channel 6	0.9973	Accepted
Channel 7	0.0020	Rejected
Channel 8	0.9992	Accepted
Channel 9	0.9972	Accepted

feature value x_i by its attenuation value $F(\gamma_i)$ and the modulated feature value $x_i F(\gamma_i)$ for the ith input entered into the network. The gate function attenuates the features before they propagate through the net so we may call these gate functions as *attenuator functions*. A simple way of identifying useful gate functions is to use sigmoidal functions with a tunable parameter, and these parameters can be learned using training data.

1) Training Method: Parameters γ_i are initialized with values that make $F(\gamma_i) = 1/(1 + e^{-\gamma_i})$ close to 0 for all i. Consequently, $x_i F(\gamma_i)$ is small at the beginning of the training, so the FSMLP *allows only a very small "fraction" of each input feature value to pass into the standard part of the MLP*. As the network is trained, it selectively allows only important features to be active by increasing their attenuator weights (and hence, increasing the multipliers of x_i associated with these weights) as dictated by the gradient descent. The training can be stopped when the network has minimum mean squared error. Features with *low* attenuator weights are eliminated from the feature set.

C. K-Means Clustering

The task of k-means clustering algorithm is to group the given data into k number of different homogeneous groups. The homogeneity is measured by similarity. Normally the k-means clustering algorithm measures similarity by the Euclidian distance. The prototype of each cluster is denoted by the cluster center. Initial cluster center may be chosen as k different data points from the given set of data. Each data point is assigned to its nearest cluster and recomputed the cluster center. The process of assignment continues until each cluster center unchanged.

TABLE II
ERROR INDEXES FOR TRAINING AND VALIDATION SET FOR THE NETWORKS ANN, ANN_FS, AND ANN_Hyb

Learning	MLPs	correlation coefficient	rmse (mm/h)
TRAINING	ANN	0.920	1.458
	ANN_FS	0.920	1.451
	ANN_Hyb	0.937	1.321
VALIDATION	ANN	0.921	2.239
	ANN_FS	0.928	2.124
	ANN_Hyb	0.954	1.694

IV. TRAINING OF THE NETWORKS AND THEIR RESULTS

A. FSMLP Training for Feature Selection

We have trained the FSMLP network five times with different initialization using the nine-feature BT data. We only consider those features whose attenuation value at the end of the run are >0.800. A "voting scheme" is then applied to see which features are selected most of the time and thus choose those features. This scheme selects seven features out of nine (Table I). Table I reveals that FSMLP rejects the 21.3-GHz channel, which is mainly responsible for the water vapor and 37.0-GHz horizontal channel. The network does not reject the 37-GHz vertical channel, which is affected by moderate types of rain. The network also gives preference to all the lower frequency channels (both vertical and horizontal polarization). This fact agrees with what is in the literature, i.e., lower frequencies are more sensitive to rain as for example the 10-GHz channel is sensitive for the strong precipitation. Further, for the 85.5-GHz frequency, where scattering effect dominates, the network has selected both the vertical and horizontal channels.

B. MLP Training for Rain Rate Estimation

Three different networks are trained for the instantaneous rain rate retrieval utilizing the BTs from TMI and PR near-surface rainfall rate.

1) MLP Without Feature Selection (ANN): First, the neural network is trained using the entire nine-channel BTs from TMI as input and the collocated PR near-surface rain rate as target. The whole dataset is divided into two parts: 80% is used for training and the rest for validation. Various network architectures are trained with different hidden layers and nodes. Network with two hidden layers having nodes 25 and 10 come out to be good enough to trace the nonlinear relations of the BTs and PR rainfall rate. Thus, the network architecture is 9-25-10-1. We have considered more hidden nodes so as to ensure that the network can adopt the nonlinearity of the input features. The above network architecture is realized in MATLAB toolbox based on Levenberg–Marquardt backpropagation algorithm. The main advantage of this algorithm is its fast convergence [12]. We named this network as ANN.

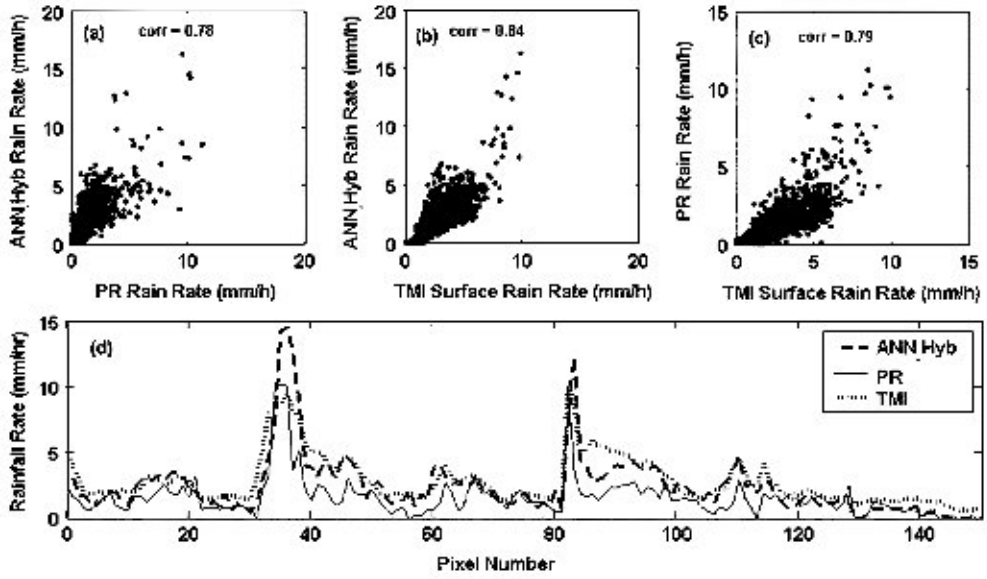

Fig. 2. Scatter plots of rain rate versus (a) ANN_Hyb and PR, (b) ANN_Hyb and TMI, (c) PR and TMI, and (d) ANN_Hyb, PR, and TMI derived rainfall rate plot with coincident pixel number on March 14, 2000.

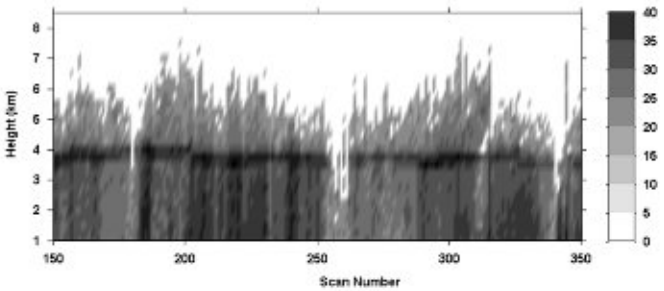

Fig. 3. Vertical cross section of corrected reflectivity factor in logarithmic power showing the bright band at around 4-km height on March 14, 2000.

2) MLP With Feature Selection (ANN_FS): The MLP network is trained by the training dataset with the seven selected features. Thus, the network architecture now becomes 7-25-10-1. Here it should be noted that the number of hidden layers and nodes are kept the same as in the case of the network without FS. We named this network ANN_FS.

3) Hybrid MLP Network (ANN_Hyb): On the selected features, k-means clustering algorithm is applied. Here we obtain two good clusters. Several MLPs for each cluster are trained with training sample and tested with a test sample. Sensitivity based on both weight matrix as well as input variations are studied, and the best MLPs for each cluster are chosen. The trained MLPs for both clusters have the configuration of 7:25:10:1. These MLPs are then combined to form a hybrid network (Fig. 1) with the objective that the hybrid network will reflect output of the best suited MLP. That means an observation of the selected features of an unknown sample will determine its cluster number and fire that MLP for rainfall estimation. This hybrid network is named as ANN_Hyb.

Various results of the training and validation of the three different networks, viz. ANN, ANN_FS, and ANN_Hyb are listed in Table II. It is observed that for the training and validation sets the correlation coefficient for ANN_Hyb network is higher compared to other two networks. In terms of root mean square error (rmse) also the ANN_Hyb network performs better.

TABLE III
COMPARISON OF ERRORS OF DIFFERENT NETWORKS WITH PR NEAR-SURFACE RAIN RATE AND TMI SURFACE RAIN RATE FOR MARCH 14, 2000 DATA

	A PR			B TMI		
Networks	correlation coefficient	rmse (mm/h)	bias (mm/h)	correlation coefficient	rmse (mm/h)	bias (mm/h)
ANN	0.701	1.376	0.374	0.750	1.174	-0.784
ANN_FS	0.783	1.282	0.687	0.848	1.033	-0.471
ANN Hyb	0.782	1.134	0.511	0.840	1.124	-0.647

V. CASE STUDY FOR RAIN RATE ESTIMATION

Two rain events from different locations are considered for this case study. One is stratiform type on March 14, 2000 over the Atlantic Ocean (34° to 36°S and 15° to 27°W) and the other having both stratiform and convective on March 21, 2000 over the Pacific Ocean (26° to 32°S and 138° to 147°W). Updated weights from ANN, ANN_FS, and ANN_Hyb networks are utilized to estimate the instantaneous rain rate from the input BTs. These estimated rain rate from the networks are compared with TRMM standard data product 2A25 (PR) and 2A12 (TMI).

The instantaneous rainfall rates on March 14, 2000 event are estimated by these three networks. The corresponding statistics with respect to rain rate derived from PR and TMI are listed in Table III(A) and (B) respectively. Table III(A) revels that the ANN_Hyb network performs better compared to other networks in terms of correlation coefficient and rmse. Here biasing is positive for all the networks, which indicates that with respect to PR standard product the estimated rain rate is overestimating. From Table III(B), it can be observed that there is negative biasing with

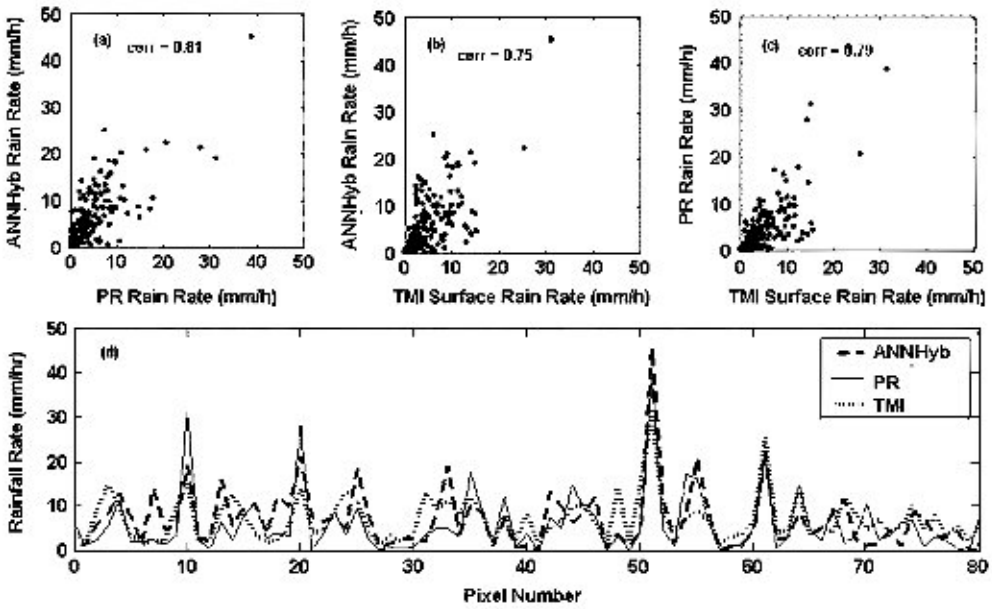

Fig. 4. Scatter plots of rain rate versus (a) ANN_Hyb and PR, (b) ANN_Hyb and TMI, (c) PR and TMI, and (d) ANN_Hyb, PR, and TMI derived rainfall rate plot with coincident pixel number on March 21, 2000.

respect to TMI rain rate, which indicates that estimated rain rate is underestimated compared to TMI. It can also be inferred that bias in ANN_Hyb versus TMI is more compared to ANN_Hyb versus PR. Fig. 2(a) and (b) shows the scatter plots of ANN_Hyb estimated rain rate versus PR and TMI surface rain rate, respectively. For this stratiform event, TMI rain rate has a biasing of 1.158 mm/h compared to PR with rmse of 1.19 mm/h and correlation coefficient of 0.79 [Fig. 2(c)]. The pixelwise comparison of rain rate from ANN_Hyb, PR, and TMI are shown in Fig. 2(d). It can be observed from this figure that the ANN_Hyb estimated rain rate is able to capture all the variations in the stratiform event where the maximum rain rate is found to be of 11.2 mm/h. Here, the TMI rain rate is overestimated with respect to PR. This may be due to the presence of bright band for this event (Fig. 3). In a recent study, Nesbitt *et al.* [13] has pointed out that over ocean the TMI rain rate is overestimated compared to PR and that it is more prominent in case of stratiform rain. In the ANN_Hyb model, as networks are trained with PR rain rate as target, so the model-derived rain rate tends to follow the PR rain rate. The TMI rain rate, therefore, has an overall overestimation compared to ANN_Hyb.

The rain event on March 21, 2000, which contains both stratiform and convective rain, maximum rain rate is observed up to 45 mm/h. Fig. 4(a)–(c) shows the scatter plots for ANN_Hyb versus PR, ANN_Hyb versus TMI, and PR versus TMI-derived rain rate, respectively. The error statistics for this event are shown in Table IV. Similar to the earlier event, ANN_Hyb estimated rain rate has positive bias with respect to PR and negative bias with respect to TMI observations. The correlation between estimated rain rate from ANN_Hyb network and PR is about 0.81 with rmse 4.15 mm/h. This increase in error is acceptable because this dataset contains BTs from convective situation also. As in convective situations, rain rate is not uniform, having updraft and downdraft. This introduces the error in rain rate estimation. For this event also, there is an overall

TABLE IV
COMPARISON OF ERRORS FOR RAIN RATES BETWEEN ANN_HYB, PR, AND TMI FOR THE MARCH 21, 2000 EVENT

	correlation coefficient	rmse (mm/h)	bias (mm/h)
ANN_Hyb Vs PR	0.814	4.164	0.956
ANN_Hyb Vs TMI	0.752	4.176	-0.605
TMI Vs PR	0.793	3.394	0.351

overestimation of TMI rain rate with respect to PR [Fig. 4(c)]. From Table IV, it can be inferred that the ANN_Hyb derived rain rate is underestimated with respect to TMI. But it is less as this event contains convective rain also. Fig. 4(d) shows the pixelwise plot of rain rate from ANN_Hyb network PR and TMI.

A. Spatial Comparison of ANN_Hyb With TMI Rain Rate

The spatial distribution of rain rate estimated from the ANN_Hyb model is compared with TMI. Fig. 5 shows the contour plots of rain rate for the TMI and ANN_Hyb models, respectively, for the March 14, 2000 event over the Atlantic Ocean. It can be inferred from the figure that the spatial structure of ANN_Hyb estimated rain rate is almost similar to that of TMI. The high rain rate area around 27°W and 33.5°S is outside the PR swath, which contains convective rain. But inside the PR swath the rain pattern is stratiform. ANN_Hyb algorithm is able to capture these high rain rate areas also.

B. Ground Validation

For the actual test of the ANN_Hyb model it is validated with an operational Doppler Weather Radar (DWR) at SHAR (13.66°N and 80.23°E), India. Two events of TRMM that overpass on November 6 and 7, 2003 have been considered where

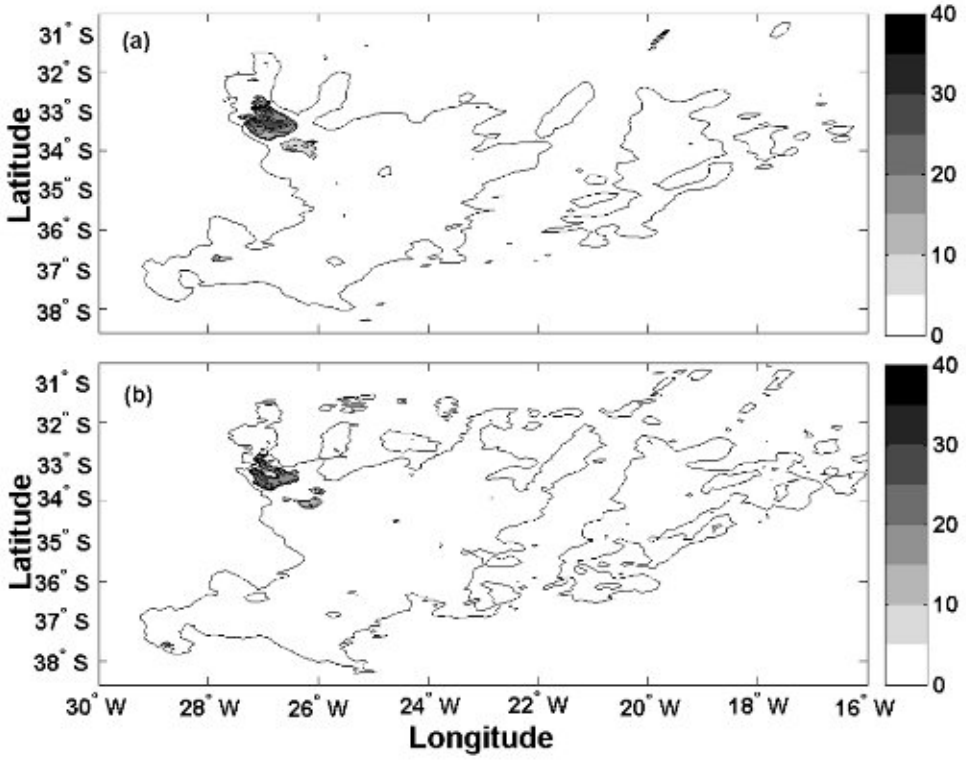

Fig. 5. Spatial plots of rain rate for (a) 2A12 algorithm and (b) ANN_Hyb algorithm.

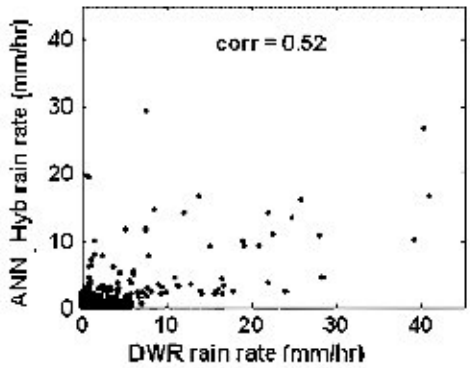

Fig. 6. Scatter plot of DWR and ANN_Hyb rain rate.

precipitation echoes were present. DWR data are averaged in $0.1^\circ \times 0.1^\circ$ grid resolution. For rainfall retrieval from DWR, two Z-R relations for convective ($Z = 209.38\ R^{1.39}$) and stratiform ($Z = 64.2\ R^{1.78}$) rain are utilized. These relations are found out from Joss–Waldvogel Disdrometer located near the radar site. Fig. 6 shows the scatter plot of DWR and ANN_Hyb rain rate for the same events. Correlation of 0.52 and rmse of 5.20 mm/h is observed for the rain rate comparison.

VI. Discussion and Conclusion

This study manifested use of a hybrid neural network model for rainfall retrieval from the TMI passive sensor onboard TRMM using online feature selection and clustering techniques. Separate ANN models have been developed with and without theses techniques. All the networks are trained to give the near-surface instantaneous rain rate. Application of the networks in this study clings to over sea only. This is because the training data considered here are comprised of BTs from MW frequencies, and over sea its response to rainfall is more compared to land, particularly for the lower frequency channels. Moreover, over land, use of lower frequency channels (which work on absorption/emission mechanism) are limited due to the high background emissivity ($\sim$0.8). Performance of the network improves for input features that are selected utilizing FSMLP algorithm. This may be due to the fact that the discarded channels do not represent very much the surface rain rate and thus produce more error in output. The k-means clustering technique has so far been used in many fields, e.g., see [14]. Results presented in this paper show good reason to incorporate FS and clustering techniques for rainfall estimation from remotely sensed data. The network developed shows flexibility for data from different locations. It is able to capture rain rate for an independent validation dataset on March 21, 2000 over the Pacific Ocean as well as for March 14, 2000 over the Atlantic Ocean. The hybrid network ANN_Hyb provided better instantaneous rain fall rate estimation compared to ANN and ANN_FS for the same events when compared with the PR and TMI surface rain rate. ANN_Hyb estimated rain rate is underestimated with respect to TMI over ocean, and it is more for the stratiform event. This is attributed to the presence of bright band. The proposed ANN_Hyb model is validated with ground-based DWR observations.

Acknowledgment

Financial support from the Department of Space, Government of India is gratefully acknowledged. The authors are thankful to the NASA Goddard Space Flight Center for providing the required data for the present work. Thanks also go

to the TSDIS help desk and Orbit Viewer team. The authors also would like to express their gratitude toward the college authority of Kohima Science College for providing the necessary facilities to carry out the research work. The authors are indebted to the two anonymous reviewers for providing very constructive comments and suggestions. The fruitful discussion with R.M. Gairola (Space Application Centre, Ahmedabad, India) is thankfully acknowledged. The authors also would like to thank S. Venkataswaralu (Director, DWR Center, India Meteorological Department, SHAR) for providing the DWR data. The authors would like to acknowledge gratefully G. Viswanathan (Director, RDC-ISRO, India) for his continuous support during the TRMM-DWR precipitation campaign and stimulating discussions on DWR systems and data format.

REFERENCES

[1] M. C. Todd, C. Kidd, D. Kniveton, and T. J. Bellerby, "A combined satellite infrared and passive microwave technique for estimation of small-scale rainfall," *J. Atmos. Oceanic Technol.*, vol. 18, pp. 742–755, 2001.

[2] R. F. Adler and A. J. Negri, "A satellite technique to estimate tropical convective and stratiform rainfall," *J. Appl. Meteorol.*, vol. 27, pp. 30–51, 1988.

[3] D. I. F. Grimes, E. Coppola, M. Verdecchia, and G. Visconti, "A neural network approach to real-time rainfall estimation for Africa using satellite data," *J. Hydrometeorol.*, vol. 4, pp. 1119–1133, 2003.

[4] K. Hsu, X. Gao, S. Sorooshian, and H. V. Gupta, "Precipitation estimation from remotely sensed information using artificial neural networks," *J. Appl. Meteorol.*, vol. 36, pp. 1176–1190, 1997.

[5] D. Tsintikidis, J. L. Haferman, E. N. Anagnostou, W. F. Krajewski, and T. F. Smith, "A neural network approach to estimating rainfall from spaceborne microwave data," *IEEE Trans. Geosci. Remote Sens.*, vol. 35, no. 5, pp. 1079–1093, Sep. 1997.

[6] T. Bellerby, M. Todd, D. Kniveton, and C. Kidd, "Rainfall estimation from a combination of TRMM precipitation radar and GOES multispectral satellite imagery through the use of an artificial neural network," *J. Appl. Meteorol.*, vol. 39, pp. 2115–2128, 2000.

[7] C. D. Kummerow, W. Barnes, T. Kozu, J. Shiue, and J. Simpson, "The Tropical Rainfall Measuring Mission (TRMM) sensor package," *J. Atmos. Oceanic Technol.*, vol. 15, pp. 809–817, 1998.

[8] C. Kummerow and L. Giglio, "A passive microwave technique for estimating rainfall and vertical structure information from space. Part I: Algorithm description," *J. Appl. Meteorol.*, vol. 33, pp. 19–34, 1994.

[9] N. Viltard, C. Kummerow, W. S. Olson, and Y. Hong, "Combined use of the radar and radiometer of TRMM to estimate the influence of drop size distribution on rain retrievals," *J. Appl. Meteorol.*, vol. 39, pp. 2103–2114, 2000.

[10] S. Haykin, *Neural Networks A Comprehensive Foundation*, 2nded, Singapore: Pearson, 2001.

[11] N. R. Pal, S. Pal, J. Das, and K. Majumdar, "SOFM-MLP: A hybrid neural network for atmospheric temperature prediction," *IEEE. Trans. Geosci. Remote Sens.*, vol. 41, no. 12, pp. 2783–2791, Dec. 2003.

[12] B. M. Wilamowski, S. Iplikci, O. Kaynak, and M. Ö. Efe, "An algorithm for fast convergence in training neural networks," in *Proc. INNS-IEEE Int. Joint Conf. on Neural Networks (IJCNN 2001)*, Washington, DC, Jul. 14–19, 2001, pp. 1778–1782.

[13] S. W. Nesbitt, E. J. Zipser, and C. D. Kummerow, "An examination of version 5 rainfall estimation from the TRMM Microwave Imager, Precipitation Radar, and rain gauges on global, regional, and storm scales," *J. Appl. Meteorol.*, vol. 43, pp. 1016–1036, 2004.

[14] C. R. Williams, W. L. Ecklund, and P. E. Johnston, "Cluster analysis to separate air motion and hydrometeors in vertical incident profiler observations," *J. Appl. Meteorol.*, vol. 17, pp. 949–962, 2000.

Diganta Kumar Sarma received the M.Sc. degree from Gauhati University, Assam, India.

He is currently a Research Fellow in Kohima Science College, Nagaland, India, under a research program sponsored by the Indian Space Research Organization. His research topic is study and retrieval of precipitation from ground and spaceborne sensors.

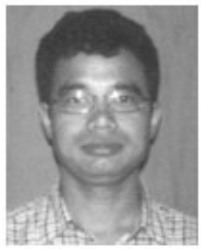

Mahen Konwar received the M.Sc. degree from the Gauhati University of Assam, Assam, India.

He is currently a Research Fellow in Kohima Science College, Nagaland, India, under a research program sponsored by the Indian Space Research Organization. His research topic is the study of convection and rain drop size distribution.

Jyotirmoy Das received the M.Tech. and Ph.D. degrees from the University of Calcutta, Calcutta, India.

He is currently the Senior Professor and the Head of Electronics and Communication Sciences Unit, Indian Statistical Institute, Calcutta. His current research interests include atmospheric science problems, computational intelligence, and millimeter wave propagation.

Dr. Das is a fellow of the National Academy of Science (Allahabad).

Srimanta Pal received the B.Sc. degree in mathematics from the University of Calcutta, Calcutta, India, in 1978, the B.Tech. (IEE) and M.B.A. degrees from Jadavpur University, Calcutta, in 1982 and 1989, respectively, the M.Tech. degree in computer science from Indian Statistical Institute, New Delhi, in 1984, and the Ph.D. degree in computer science from the Indian Institute of Technology, Kharagpur, in 1992.

Sanjay Sharma received the M.Sc. and Ph.D. degrees from Gauhati University, Assam, India.

He was a Junior Associate Member of AS-ICTP Trieste, Italy from 1997 to 2000. His current research interest includes satellite and radar meteorology. Presently he is a faculty member in the Department of Physics, Kohima Science College, Kohima, India.